

Analytical Methods

Accepted Manuscript



This is an *Accepted Manuscript*, which has been through the Royal Society of Chemistry peer review process and has been accepted for publication.

Accepted Manuscripts are published online shortly after acceptance, before technical editing, formatting and proof reading. Using this free service, authors can make their results available to the community, in citable form, before we publish the edited article. We will replace this *Accepted Manuscript* with the edited and formatted *Advance Article* as soon as it is available.

You can find more information about *Accepted Manuscripts* in the [Information for Authors](#).

Please note that technical editing may introduce minor changes to the text and/or graphics, which may alter content. The journal's standard [Terms & Conditions](#) and the [Ethical guidelines](#) still apply. In no event shall the Royal Society of Chemistry be held responsible for any errors or omissions in this *Accepted Manuscript* or any consequences arising from the use of any information it contains.

ARTICLE

Quantification Signalling via Transition of Solution Inhomogeneity: Determination of Iron Contents in Human Serum by the Naked Eye

Chun-Ting Kuo,^{a,c} Cheng-Han Lin,^a Yi-Ann Lii,^a Mong-Wen Gu,^a Chih-Wen Pao,^b Jyh-Fu Lee^{*b} and Chun-hsien Chen^{*a}

Cite this: DOI: 10.1039/x0xx00000x

Received 00th January 2012,
Accepted 00th January 2012

DOI: 10.1039/x0xx00000x

www.rsc.org/Analytical Methods

Visual detection triggered by sensing events has been one of the central themes in contemporary chemistry. Demonstrated here is that phase transition can successfully signal the concentration levels of analyte. The proof-of-concept example is a rapid screening scheme which allows the visual determination of whether the amount of iron(III) in the sample falls into a diagnostic concentration range by the naked eye. The screening scheme is achieved by utilizing iron–ligands polymerisation followed by the formation of flocculates that cause phase segregation, whose rate is dependent on the concentration of iron ions. The assay solution appears homogeneous until the iron(III) introduced reaches a concentration threshold, triggering the formation of heterogeneous flocculates. The two-phase assay is demonstrated enabling the determination of the diagnostic range of iron(III) concentration for human serum samples (10–35 μM , equivalent to 0.56–1.95 ppm). With a handy laser pointer, semi-quantification of sub-ppm (μM -level) iron(III) can be picked up conveniently by the naked eye through the Tyndall effect, in which the light is scattered by colloidal suspension. By carefully selecting the experimental conditions, the visual sensing method can be applied to iron(III) detection in serum in 1 min. For example, a 5.4-fold diluted serum samples in which the iron(III) concentration as low as 4.7 μM (0.26 ppm) can be determined visually. The sensing mechanism of flocculation is elucidated *via* a series of characterisations.

Introduction

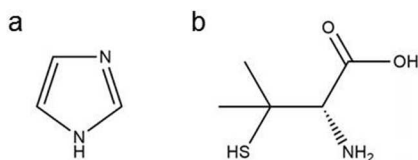
Iron is one of the most abundant transition metal ions in human bodies and an indispensable composition in enzymes such as myoglobin, cytochrome, and catalase.^{1,2} An adult male requires around 1 mg per day whereas a menstruating female requires about 1.4 mg per day.² The serum iron concentration in a healthy human body falls in the range of 10–35 μM (equivalent to 0.56–1.95 ppm).³ Iron deficiency or overload is a common problem that may pose threat to human health. For instance, iron deficiency may give rise to anemia and coronary artery disease. A recent discovery also indicates that the iron deficiency is a potential risk factor for cardiovascular and rheumatoid arthritis.⁴ Hemochromatosis, a hereditary disorder, causes the accumulation of excess iron ions in tissues and leads to liver damage, kidney failure, or even death.⁵ Hence, it is of great significance to determine whether the amount of iron falls into a diagnostic concentration range.

Atomic spectroscopy, electrochemistry, fluorescence spectroscopy, and colourimetry are prevailing methods for detecting the concentration of iron ions. Atomic spectroscopy includes atomic absorption spectrometry (AAS),^{2,6} inductively coupled plasma atomic emission spectrometry (ICP-AES),⁷ and inductively coupled plasma mass spectrometry (ICP-MS),⁸

which are of high precision, high sensitivity, and low detection limits below nM. Electrochemistry is employed to determine the concentration of iron ions by inducing redox reaction and collecting the current as signal.⁹ In fluorescence spectroscopy, the concentration of iron ions is determined by measuring the fluorescence emitted from Fe-fluorophore complexes. In Cabantchik's study,¹⁰ for example, the presence of Fe^{3+} quenches the fluorophore so that the reduction of fluorescent intensity corresponds to the concentration of Fe^{3+} . Although numerous studies have employed fluorescent nanomaterials to improve the sensitivity of iron ions detection,^{11–13} synthesis of nanomaterials and the need for fluorescence spectrometers render these methods not readily available. In the lack of spectrometers, colourimetry is employed to enable the naked eye to estimate the ballpark amount of iron ions by the intensity difference. For example, Pitchumani and co-workers¹⁴ developed a method that allows visual detection of Fe^{3+} with the employment of *per*-6-amino- β -cyclodextrin as a supramolecular host for Fe^{3+} and *p*-nitrophenol as a spectroscopic probe. With the addition of 50 μM Fe^{3+} , the solution with chemosensors turned from intense yellow to colourless.¹⁴ The fly in the ointment in Pitchumani's study was that the samples were simply prepared in pure water and the quantitative measurements required a UV-vis spectrometer. To

improve the sensitivity of colourimetry, gold nanoparticles were used for a distinct colour change caused from the particle aggregation triggered by analytes.^{15,16} However, a UV-vis spectrometer was still necessary for analytes detection on a μM scale.¹⁷ For most clinical applications, the important information is whether the amount of iron ions falls into a diagnostic concentration range rather than the precise quantity. Therefore, it is of great importance to develop an instrument-free method that enables quantitative determination of the iron deficiency or overload with the naked eye.

In this study, we develop a rapid visual screening scheme for Fe^{3+} in human serum. Without any instruments, this visual detection of the analyte is accomplished in 1 min *via* phase segregation driven by polymerisation. Our experimental design is based on the well-known bonding of Fe^{3+} to ligands with chelating sites such as iron–nitrogen in the cases of pyrrole moieties (*e.g.*, iron porphyrins)^{18,19} or iron/histidine-containing enzymes.²⁰ Therefore, imidazole (Scheme 1a) was used not only as a buffer but also as a chelating ligand. The presence of Fe^{3+} is brought into visualisation by the formation of an inhomogeneous phase in about 20 min. Among the typical metal ions found in serum, Cu^{2+} requires particular attentions because it exhibits chelation with imidazole^{21,22} and reactivity with thiol-containing amino acids.^{23–26} To circumvent the potential interference caused by Cu^{2+} which has roughly equal amount as Fe^{3+} in human serum,⁸ employed to chelate Cu^{2+} herein is penicillamine (Scheme 1b), a therapeutic agent for Wilson's disease^{27,28} caused by the abnormal accumulation of Cu^{2+} in human organs. Surprisingly, penicillamine not only chelates Cu^{2+} but also undergoes a cooperative effect with Cu^{2+} to accelerate the Fe^{3+} -sensing event. As a result, the determination of Fe^{3+} *via* the inhomogeneous phase takes only 1 min. It should be noted that penicillamine is not among the necessary amino acids and does not exist in human serum. To detect the Fe^{3+} concentration level in human serum by the naked eye, the detecting range of the rapid screening is further improved from mM to μM assisted by the laser beam from a handy laser pointer to induce the Tyndall effect, in which the light is scattered by the flocculated suspension. In the later section of this manuscript, the mechanism of flocculation and the cooperative effect caused by penicillamine and Cu^{2+} are revealed. Possible structures of flocculates are proposed based on the X-ray absorption spectra.



Scheme 1 Chemical structures of (a) imidazole and (b) D-penicillamine.

Results

Semi-quantification of iron(III)

Figure 1 shows that the assay solution (left vial) containing imidazole buffer and penicillamine stays clear and that the presence of Fe^{3+} can be conveniently determined by the naked eye from the formation of yellowish flocculates (right vial) in 1 min. The detection of Fe^{3+} is carried out without using any dye or metal nanoparticle. To make the flocculates apparent for the photographs, at the beginning of this Result Section, the quantity of Fe^{3+} prepared in Figure 1 was made about 20 folds

higher than that in human serum. The clearance-flocculation boundary for the visual quantification of Fe^{3+} can be adjusted by the amount of penicillamine in the assay. A larger amount of penicillamine delays the flocculation formation (*vide infra*). Cu^{2+} is added into the sample solution to imitate human serum^{8,29} in which the concentrations of Fe^{3+} and Cu^{2+} are on the same order of magnitude with the former ($[\text{Fe}^{3+}] \sim 10\text{--}35 \mu\text{M}$ or $0.56\text{--}1.95 \text{ ppm}$)³ being typically larger than the latter ($[\text{Cu}^{2+}] \sim 16\text{--}24 \mu\text{M}$ or $1.02\text{--}1.52 \text{ ppm}$).³⁰

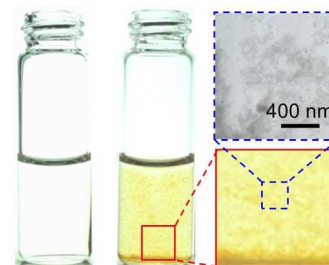


Fig. 1 Determination of Fe^{3+} *via* phase segregation. The assay solution (left vial) appears clear while the yellow flocculates form in the presence of both Fe^{3+} and Cu^{2+} (right vial). Cu^{2+} alone does not form flocculates in the assay solution. The lower and upper insets show a magnified photograph and a TEM image of the yellow flocculates, respectively. Assay solution: 18.5 mM imidazole buffer (pH 6.20) and 0.74 mM penicillamine; sample solution: 0.46 mM Fe^{3+} and 0.31 mM Cu^{2+} . The amount of penicillamine is large enough to completely chelate Cu^{2+} . Here, the concentrations of Fe^{3+} and Cu^{2+} are nearly an order of magnitude larger than those found in human serum^{8,29,30} to provide a distinguished morphology of the flocculates. The photograph of vials was obtained 1 min after the sample was introduced. Note that the introduced aliquot of Fe^{3+} was prepared freshly to avoid the formation of iron(III) oxide-hydroxides.

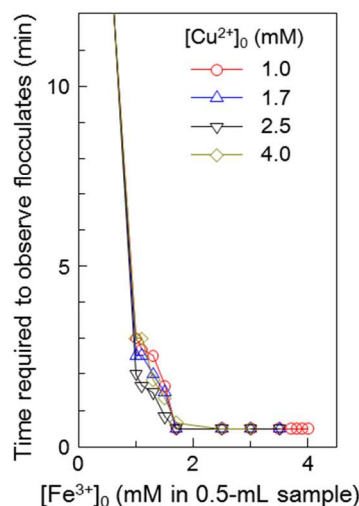


Fig. 2 Time required to exhibit observable flocculates as a function of concentrations of Fe^{3+} and Cu^{2+} . $[\text{Fe}^{3+}]_0$ and $[\text{Cu}^{2+}]_0$ ranged from 0.5–4.0 mM and 1.0–4.0 mM, respectively, in the 0.5-mL aliquot of sample solutions. Specifically, the final concentrations of Fe^{3+} and Cu^{2+} in the cuvettes with 2.7 mL solution were diluted by 27/5 fold. For $[\text{Fe}^{3+}]_0$ below a certain level (*e.g.*, $\sim 1.0 \text{ mM}$), the solution remained clear for a long time ($> 30 \text{ min}$) which was outside the vertical frame of this Figure. Other experimental conditions are the same as described in Figure 1. The concentrations are higher than those of real samples (see Figure 3) because the purpose of this experimental result is to present the correlation between the rate of flocculation and the amount of analyte.

The formation of insoluble flocculates may be ascribed to the polymerisation of Fe^{3+} -ligand complexes or the reduction of Fe^{3+} to Fe^0 particles. To further identify the source behind flocculates, a TEM micrograph (transmission electron

microscope, Figure 1) was taken, in which the weak contrast and loose structure of the flocculates supports polymerisation rather than the development of Fe⁰-containing nanoparticles. A detailed mechanism of flocculation will be included in the Discussion Section.

To explore the practicality of this concentration screening of Fe³⁺, the rate of flocculation is recorded as a function of [Fe³⁺]₀, in which the subscript denotes the concentration of Fe³⁺ from the stock or sample solution prior to being introduced to the assay solution. As shown in Figure 2, for [Fe³⁺]₀ below a certain level (*e.g.*, *ca.* 1.0 mM), the solution remains clear for a very long time (*e.g.*, > 30 min). The time required for the flocculates to form decreases with the increasing [Fe³⁺]₀. The [Fe³⁺]₀-dependent flocculation ensures the success of the Fe³⁺ semi-quantification. Concerning the use of penicillamine to chelate Cu²⁺ in human serum, a potential interference caused by the redox reaction between Cu²⁺ and the thiol group of penicillamine needs to be clarified.²³ Therefore, the effect brought by different concentrations of Cu²⁺ is also examined for the semi-quantification. Figure 2 shows that the time required for the flocculates to form is not affected by [Cu²⁺]₀. It should be noted that, without the presence of Fe³⁺, Cu²⁺ alone does not form flocculates in the assay solution containing imidazole and penicillamine (*vide infra*). The behaviours of flocculation observed in Figures 1 and 2 ensure the promising application of this semi-quantification of Fe³⁺ in human serum.

Analysis of human serum samples with the help of a laser pointer

The concentration of Fe³⁺ in human serum samples is typically found to be 10–35 μM (0.56–1.95 ppm),³ about one twentieth of the amounts introduced in Figure 1. Such low concentration of Fe³⁺ makes the observation of the flocculation challenging by the naked eye. To facilitate the visual determination, Tyndall effect is integrated in the detection scheme to intensify the visibility of trace flocculates by employing a common laser pointer (see a demo video clip in ESI). For the imitated human serum samples displayed in Figure 3a, a green beam resulting from the Tyndall effect was shown in the sample containing 20.0-μM (1.12 ppm) Fe³⁺ while absent in the iron-deficient one with only 8.0-μM (0.45 ppm) Fe³⁺. The presence or absence of a beam path makes it easy to distinguish the normal serum sample from the Fe³⁺-deficiency one. For standard reference materials (Trace Elements Serum L-1, SeronormTM, see Experimental) as shown in Figure 3b, the green beam passing the normal sample (25.6 μM or 1.43 ppm Fe³⁺, determined by ICP-AES) is certainly distinguishable from that of the iron-deficient sample (8.5 μM or 0.47 ppm Fe³⁺, prepared by dilution of the normal sample). The result verifies the applications in human serum containing potential interferants. For those exhibiting flocculates, the iron levels could be normal (10–35 μM or 0.56–1.95 ppm) or overloaded (> 35 μM or 1.95 ppm) because both cases exhibit flocculates and are indistinguishable. Therefore, it is required to have a second assay which dilutes the sample and shifts the clearance-flocculation boundary. Specifically, with a second assay using another 3.5-fold dilution of the samples, test results of clear solution and phase-segregated one correspond to normal and overloaded level, respectively.

Discussion

Key components of the flocculates

The visual sensing system is comprised of Fe³⁺, Cu²⁺, penicillamine, and imidazole buffer. To determine which of the four substances dominates the formation of the flocculates, the rates of flocculation in a complete system and other incomplete systems without one or two substances are tabulated in Table 1. Although the concentrations of the substances, especially the ratio of [Fe³⁺]₀ to [Cu²⁺]₀, do not follow the recipe applied on the determination of human serum (Figure 3), the results can describe the flocculation occurs in both concentrated (Figure 1) and traced conditions (Figure 3) because Figure S2 shows that the flocculation behaves the same in a wide range of [Fe³⁺]₀/[Cu²⁺]₀. No flocculates were observed in the absence of either Fe³⁺ (Entries 1–4) or imidazole (Entries 2, 5–7), indicating that both Fe³⁺ and imidazole are essential components of the flocculates. The coexistence of imidazole and Fe³⁺ (Entry 8) results in observable flocculates in 20 min. The time required to find flocculates is not affected by the presence of Cu²⁺ (Entry 9) but is retarded by penicillamine (Entry 10, without Cu²⁺). Entry 10 delivers a strong implication that penicillamine is the key element of adjusting the response time and diagnostic level of Fe³⁺. Comparing Entries 8 and 11, the formation of flocculates only requires Fe³⁺ and imidazole buffer, yet the addition of penicillamine and Cu²⁺ greatly accelerates the course of sensing from 20 min to 1 min. In the following discussion, we will first look into the mechanism of flocculation *via* Fe³⁺ and imidazole, and then we will take the effects of Cu²⁺ and penicillamine into account.

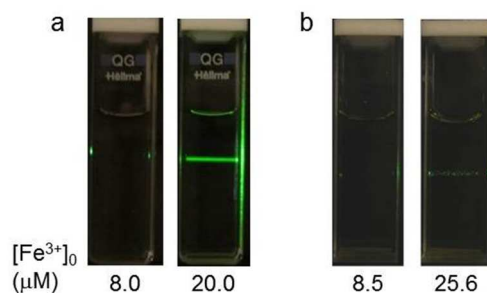


Fig. 3 Photographs of the Tyndall effect in (a) imitated and (b) real human serum sample (SeronormTM, a standard reference material). Numbers shown under the vials indicate [Fe³⁺]₀ (μM) in the introduced 0.50-mL sample aliquot. The range of iron level in human serum is 10–35 μM (0.56–1.95 ppm) for healthy adults.³ The concentration of Fe³⁺ in the real human serum sample was determined by ICP-AES and found to be 25.6 μM (1.43 ppm). The final volume in the vials was 2.7 mL, demonstrating that the presence of iron(III) concentration of 4.7 μM (0.26 ppm) in the total 2.7 mL solution can be determined by the naked eye. The Tyndall effect can be observed with a normal [Fe³⁺]₀, but no beam path was shown when [Fe³⁺]₀ was lower than the lower limit of the diagnostic concentration range. The results show that the concentration levels of other species in human serum would not cause serious interference to this sensing scheme. Concentrations of metal ions in the 0.50-mL imitated serum sample aliquot: Na⁺, 100 mM; K⁺, 5 mM; Ca²⁺, 2.5 mM; Mg²⁺, 1 mM; Cu²⁺, 20 μM; Zn²⁺, 13 μM; Ni²⁺, 0.7 μM; Cr²⁺, 0.4 μM.^{29,31} The concentration of penicillamine in the final 2.7 mL solution was 5.9 μM and the solution was buffered to pH 6.20 by 18.5-mM imidazole. The photographs were obtained at 1 min after sample introduction.

Table 1. Determination of the major reactants involved in flocculation.

Substance ^a	Entry No.										
	1	2	3	4	5	6	7	8	9	10	11
Fe ³⁺	×	×	×	×	Y	Y	Y	Y	Y	Y	Y
imidazole	Y	×	Y	Y	×	×	×	Y	Y	Y	Y
Cu ²⁺	Y	Y	×	Y	Y	×	Y	×	Y	×	Y
penicillamine	Y	Y	Y	×	Y	Y	×	×	×	Y	Y
Time (min) ^b	∞	∞	∞	∞	∞	∞	∞	20	20	30	1

^a The concentrations of substances are the same as described in Figure 1. Y and × denote, respectively, the presence and absence of the substance in the assay. The pH is maintained at 6.20 in all cases. ^b The time required for the flocculates to become observable by the naked eye.

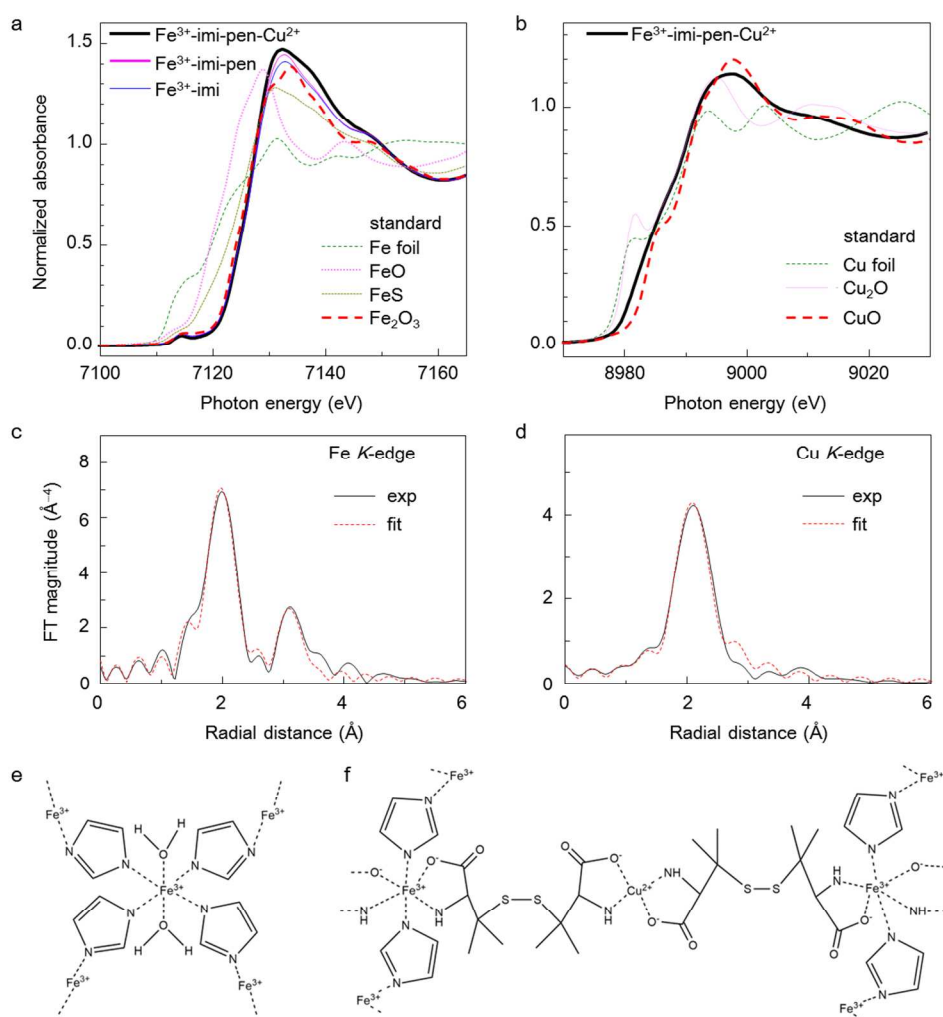


Fig. 4 X-ray absorption spectra and plausible structures of the flocculates. (a) Fe and (b) Cu K-edge XANES spectra obtained from various flocculates and standards. The Fourier transformed EXAFS spectra of (c) Fe and (d) Cu K-edge obtained from the flocculates formed with the recipes shown in Entry 11 of Table 1. The black and red curves indicate the measured and fitted results, respectively. Possible structures of the flocculates formed (e) without (Entries 8–10) and (f) with the coexistence of Cu²⁺ and penicillamine (Entry 11 of Table 1) to exemplify the structural information from the X-ray absorption techniques. The experimental conditions are the same as shown in Figure 1 with the total amounts being 10 folds to collect sufficient sample for the measurements. For the same reason, the flocculates were collected at 20 min after the sample was introduced.

ARTICLE

Characterisation of the flocculates

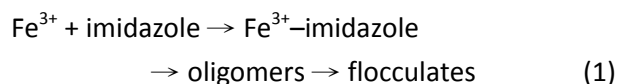
XANES (X-ray Absorption Near-Edge Structure) and EXAFS (Extended X-ray Absorption Fine Structure) data can provide the information on the valence states and coordination geometry of selected elements.³² Herein, the X-ray absorption techniques were utilised to explore the coordination of iron and copper ions in the flocculates. The information is helpful toward exploring the structure of flocculates and the mechanism of flocculation. The absorption edge energies of iron and copper are around 7120 eV³³ and 8985 eV,³⁴ respectively. A larger value of the edge energy indicates a more positively charged ion. In this study, Fe foil, FeO, FeS, Fe₂O₃, and Cu foil, Cu₂O, and CuO were employed as the reference standards. By comparing the absorption edge positions of the samples and standards, charge information of the samples is revealed. As shown in Figure 4a, the Fe K-edge XANES spectrum of the flocculates that formed in the presence of Fe³⁺ and imidazole is distinct from those of metal iron and iron(II) standards but similar to that of Fe₂O₃, iron(III), regardless of the presence of penicillamine and Cu²⁺ (Entries 8, 10, and 11). This result reveals that, for all conditions examined, iron ions in the flocculates carry the same oxidation state, Fe³⁺. The Cu K-edge XANES spectrum of the flocculates that formed with the recipes of Entry 11 is similar to that of CuO (Figure 4b). The evidence indicates that Fe³⁺ and Cu²⁺ maintain their original valence state in the flocculates even though redox reactions might take place during flocculation.

EXAFS corresponds to the X-ray absorption spectrum at around 40–1000 eV above the absorption edge.³² The EXAFS oscillation in this energy range is caused by the inference between the outgoing photoelectron wave from the target atom and that backscattered by surrounding atoms. This allows information about coordination of target atoms to be extracted.³² Fourier transformation of EXAFS yields a radial distribution function for a better understanding of the coordination (Panels c and d in Figure 4). Figure 4c shows the corresponding Fe K-edge EXAFS spectra obtained under each of the distinct condition as follows: Fe³⁺-imidazole, Fe³⁺-imidazole-penicillamine, and Fe³⁺-imidazole-penicillamine-Cu (Entries 8, 10, and 11, for clarity, only one measured spectrum is shown because all the spectra are similar). Also shown in Figure 4c is the fitting result based on the coordination number 6 of Fe³⁺-N ligation in the flocculates. The peak at ~2.0 Å in Figure 4c is consistent with the bond length of Fe³⁺-N (2.0–2.2 Å) in most iron-imidazole complexes.^{35,36} Because the nuclear charges of nitrogen and oxygen atoms are similar, EXAFS contributions from neighbouring N and O atoms are indistinguishable so that the bonding of Fe³⁺ with water and carboxyl group (if available) cannot be ruled out. The peak at 3.1 Å in Figure 4c corresponds to the Fe-Fe bond length found in Fe₂O₃,³⁷ which may result from the long-term exposure of the flocculates in air and under X-ray radiation and hence might be unrelated to the structure of flocculates. The signal of Cu K-edge EXAFS absorption can only be detected from the flocculates formed with the substances listed in Entry 11,

indicative of a structural difference between the flocculates formed with the recipes shown in Entries 8–10 and that in Entry 11. The flocculates formed in Entry 11 appear larger and more pronounced than those in Entries 8–10. According to the Cu K-edge EXAFS spectra (Figure 4d), the simulation based on the coordination geometry of N-Cu²⁺-O ligation best describes the coordination of Cu²⁺ in the flocculates. The peak at 2.1 Å in Figure 4d contributes to the bond length of Cu²⁺-N (2.2 Å) and Cu²⁺-O (2.0 Å).³⁸ Panels e and f of Figure 4 display plausible structures of the flocculates formed, respectively, in the conditions included in Entries 8–10 (two components: imidazole and Fe³⁺) and in Entry 11 (all four components: imidazole, Fe³⁺, penicillamine, and Cu²⁺). In Figure 4f, the 2-to-1 complexation of penicillamine disulphide to Cu²⁺ has been proposed by Laurie and co-workers.³⁹ ICP-AES shows that the amount of Fe³⁺ in the flocculates is 6 times that of Cu²⁺. Therefore, Figure 4f does not imply the actual stoichiometry and is only depicted to illustrate the simulation results. Other cross-linking structures consistent with the results of XANES and EXAFS are not ruled out.

Mechanistic study of flocculation: the role of imidazole

To aid in our investigations into the mechanism of flocculation, we started off by studying the simplest system shown in Entry 8 where Cu²⁺ and penicillamine are absent. Based on the EXAFS results (Figure 4c), the addition of Fe³⁺ into the imidazole buffer may initiate Fe³⁺-imidazole coordination reaction. The other nitrogen atom of imidazole is free and ready to coordinate with another Fe³⁺ ion. Flocculation may be a result of the polymerisation of the two reagents shown in Equation 1.



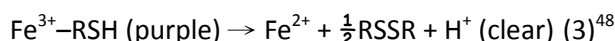
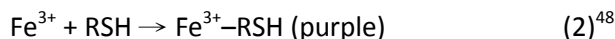
Literature reports^{40,41} by groups of Lambert and Policar show that deprotonation of a coordinated imidazole induces spontaneous polymerisation of Fe³⁺-containing complexes because the deprotonated imidazole acts as a bidentate ligand that can connect neighbouring metal ions to form a network.⁴² Similar framework structures were reported in which Fe²⁺ was coordinated tetrahedrally or octahedrally through imidazolate ions.⁴³ To confirm the proposed reaction of Equation 1, examined in this study includes the solution pH to scrutinise the effect of imidazole deprotonation. Our protocols presented in Figure 3 have the solution buffered at pH 6.20, in which imidazole is expected to slightly deprotonate according to its pKa value of 6.99.⁴⁴ We found that a higher pH environment reduces the time spent to observe the flocculation (Figure S1a). This observation is consistent with the mechanism that the more basic the environment is (higher pH), the more deprotonated imidazole as well as the flocculates appear. Deprotonation of imidazole generates a negative charge, which facilitates to compensate the positive charge of Fe³⁺-containing oligomers, and could be a driving force of polymerisation. In addition, the attractive force between Fe³⁺ and imidazole might have come from the electron affinity due to the lone pair

electrons of nitrogen or the negative charge caused by deprotonation of amide. The importance of the bidentate property of imidazole is confirmed by that the flocculates do not develop when imidazole is replaced with pyridine. Although pyridine forms complexes with Fe^{3+} ,⁴⁵ the lack of the second coordinate site limits its polymerisation.

High ionic strengths and elevated temperatures also speed up the rate of flocculation (Panels b and c of Figure S1), in a good agreement with the characteristics of polymerisation reactions.^{46,47} With a high ionic strength, the surface charge (originally 22.7 (\pm 1.5) mV, measured by a zeta potential meter) of the small flocculates that formed initially was shielded so that the small flocculates could aggregate more easily. At a higher temperature, molecules are able to overcome the activation energy more readily. From the fact that the flocculation depends on solution pH, ionic strength, and temperature, the detection range of the semi-quantification can be tuned by the three parameters above.

The role of penicillamine

Next, we focus on the reactions that involve penicillamine. The addition of penicillamine causes a temporary purple colour and a slight delay in flocculation. The purple colour is due to the formation of Fe^{3+} -penicillamine complex as shown in Equation 2, and the subsequent disappearance of the colour is attributed to the well-known redox reaction in which Fe^{3+} is reduced by penicillamine as shown in Equation 3.



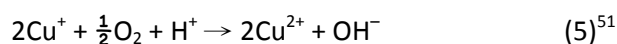
where RSH indicates penicillamine bearing an -SH group and RSSR stands for penicillamine disulphide.

To confirm Equation 3 in our experiment, the presence of Fe^{2+} is tested by ferrozine ($\text{C}_{20}\text{H}_{13}\text{N}_4\text{NaO}_6\text{S}_2$), an iron(II)-specific chelator. Immediately after adding ferrozine to a mixture of Fe^{3+} and penicillamine, a significant absorption peak at 562 nm appears in the spectra (Figure S3a), corresponding to the formation of $[\text{Fe}(\text{C}_{20}\text{H}_{12}\text{N}_4\text{O}_6\text{S}_2)_3]^{4-}$, a Fe^{2+} -ferrozine complex.¹ The same Fe^{2+} -ferrozine absorption peak is also observed when the imidazole buffer participates in the reaction (Figure S3b), but it is not detected in the absence of penicillamine (data not shown). The results verify Equation 3 as long as Fe^{3+} and penicillamine are both present. However, Equation 3 does not favour flocculation because more time is required for the flocculates to be observable, as can be seen from the time difference in Entries 8 and 10 where penicillamine delays the flocculation by 10 min. As mentioned above, the main components of the flocculates are Fe^{3+} and imidazole. The addition of penicillamine reduces Fe^{3+} to Fe^{2+} , which supposedly does not prefer to bind with imidazole due to the loss of a positive charge. As a result, flocculation does not proceed until Fe^{2+} is re-oxidised to Fe^{3+} with the help of dissolved oxygen in the sample solution.⁴⁹ The assumption is justified because, when nitrogen was bubbled into the sample solution to remove dissolved oxygen, the solution prepared as described in Entry 10 remained clear over 1 hr (data not shown).

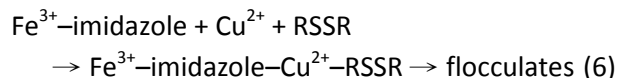
The collaborative effect of copper(II) and penicillamine

Finally, we investigated the mechanism of Entry 11 which exhibits the fastest rate of flocculation and is optimised as the detection protocol. Although the concentration ratio of Fe^{3+} to

Cu^{2+} (1.5:1) in Entry 11 may not be exactly the same as that in human serum, the behaviours are comparable because the rapid flocculation occurs in a wide range of $[\text{Fe}^{3+}]_0/[\text{Cu}^{2+}]_0$ as shown in Figure S2. In addition, ferrozine is employed to probe the product of penicillamine oxidation. UV-vis spectra (Figure S3c) show no indication of Fe^{2+} -ferrozine complex (at 562 nm), yet a slight increase at 470 nm, ascribed to $[\text{Cu}(\text{ferrozine})_2]^{3-}$ complex by a recent study.⁵⁰ This result indicates that penicillamine reacts with Cu^{2+} more facily than with Fe^{3+} . Penicillamine is known to be oxidised by Cu^{2+} (Equation 4).²³ The resulted Cu^+ will be re-oxidised to Cu^{2+} by dissolved oxygen (Equation 5) and will then react with penicillamine again. Although the amount of penicillamine is greater than Cu^{2+} in our study, the recyclable Cu^{2+} will exhaust the remaining penicillamine. Therefore, the absence of Fe^{2+} in Figure S3c can be attributed to the depletion of penicillamine by Cu^{2+} .



A Cu^+ -specific chelator, bcs (bathocuproinedisulfonic acid disodium salt, $\text{C}_{26}\text{H}_{18}\text{N}_2\text{Na}_2\text{O}_6\text{S}_2$),⁵² was used to justify Equation 4 in our experimental conditions (Figure S4). By combining the results of Figure S3c, it is conclusive that penicillamine favours the reduction of Cu^{2+} when Cu^{2+} and Fe^{3+} are both present.⁵³ After Cu^{2+} is reduced by penicillamine, Cu^{2+} can be recovered by O_2 and then speed up the flocculation by acting as a linking component within the polymers (Figure 4f). This hypothesis is supported by two experimental results: 1) instead of Cu^+ , Cu^{2+} is detected in the flocculates *via* XANES; 2) the flocculates do not form within 1 min in the anaerobic experiments. Cu^{2+} not only prevents Fe^{3+} from being reduced by penicillamine but also assists flocculation. Most important of all, the produced penicillamine disulphide *via* Cu^{2+} may be critical to the acceleration of flocculation (Entry 11) because the four coordinating sites for metal ions are helpful in forming a metal-ligand network.³⁹ This hypothesis was proven valid because the addition of Cu^{2+} or penicillamine alone does not facilitate flocculation (Entries 9 and 10). Moreover, literature reports show that ascorbic acid is able to reduce disulphides of small molecules and protein disulphides.⁵⁴⁻⁵⁷ The crucial role of cross-linking made by penicillamine disulphide is further verified by ascorbic acid which reduces the disulphide bonds and resulted in clear solution due to the dissolution of the flocculates (Figure S5). Accordingly, the following mechanism is proposed: in the presence of Cu^{2+} and penicillamine, the oxidised disulphide binds to Fe^{3+} and Cu^{2+} to form a larger complex with the aid of imidazole (Figure 4f),³⁹ enabling the flocculates to be observable within 1 min. The mechanism is shown as Equation 6.



Conclusions

In this manuscript, we show that the homogeneity-to-flocculation transformation of the assay can determine visually the concentration levels for Fe^{3+} in human serum samples. In cases where $[\text{Fe}^{3+}]_0$ is higher than the lower limit of the diagnostic concentration range (micromolar level, Figure 3b),

fluffy flocculates are formed within one minute and can be observed by the naked eye with the help of a handy laser pointer. The detection range of $[\text{Fe}^{3+}]_0$ is tunable by changing the solution volume, pH, ionic strength, and temperature. We reveal the mechanism of the flocculation, which involves the binding between Fe^{3+} , imidazole, Cu^{2+} , and penicillamine disulphide produced from the redox reaction between Cu^{2+} and penicillamine. The significant advantage of this method lies in its instrument-free nature and the semi-quantification sense. To determine whether the analyte falls in a diagnostic concentration range, this phase-transition approach is more conclusive than the prevailing colourimetry in which the degree of colour intensity is difficult to decide visually.

Acknowledgements

The authors thank MOST (Taiwan, 101-2628-M-002-012, 101-2113-M-002-001-MY2), NTU (102R890911), and AOARD for the financial support. Thanks to National Synchrotron Radiation Research Centre (NSRRC) for the support of XANES and EXAFS measurements. Thanks also to Ms. Fang-Mei Chen for the manuscript preparation and to Ms. S.-J. Ji and C.-Y. Chien of Precious Instrument Centre (NTU) for TEM measurements.

Notes and references

^a Department of Chemistry and Centre for Emerging Material and Advanced Devices, National Taiwan University, Taipei, Taiwan 10617; E-mail: chhchen@ntu.edu.tw

^b National Synchrotron Radiation Research Centre, Hsinchu, Taiwan 30076; E-mail: jflee@nsrrc.org.tw.

^c Present address: Department of Chemistry, University of Washington, Seattle, WA 98195-1700, USA.

[†] Electronic Supplementary Information (ESI) available: details of experimental procedures. The effects of $[\text{Fe}^{3+}]_0/[\text{Cu}^{2+}]_0$, pH, temperature, and ionic strength on the flocculation formation. The determinations of Fe^{2+} , Cu^+ , and penicillamine disulphide in the flocculates. A video clip demonstrating the formation of flocculates observed via Tyndall effect. See DOI:10.1039/b000000x/

1. D. C. Harris *J. Chem. Educ.* **1978**, *55*, 539-540.
2. H. Z. Şenyuva; D. Y. Sarica; T. Özden *Turk. J. Chem.* **2002**, *26*, 425-430.
3. P. Che; J. Xu; H. Shi; Y. Ma *J. Chromatogr. B* **1995**, *669*, 45-51.
4. A. M. Stoyanova; V. P. Michailov; A. A. Alexiev *Bull. Chem. Technol. Macedonia* **2000**, *19*, 35-40.
5. K. J. Allen; L. C. Gurrin; C. C. Constantine; N. J. Osborne; M. B. Delatycki; A. J. Nicoll; C. E. McLaren; M. Bahlo; A. E. Nisselle; C. D. Vulpe, et al. *N. Engl. J. Med.* **2008**, *358*, 221-230.
6. M. T. Glenn; J. Savory *Anal. Chem.* **1973**, *45*, 203-205.
7. R. Selvaraju; R. G. Raman; R. Narayanaswamy; R. Valliappan; R. Baskaran *Romanian J. Biophys.* **2009**, *19*, 35-42.
8. H. Vanhoe; C. Vandecasteele; J. Versieck; R. Dams *Anal. Chem.* **1989**, *61*, 1851-1857.
9. E. Wang; A. Liu *Microchem. J.* **1991**, *43*, 191-197.
10. S. D. Lytton; B. Mester; J. Libman; A. Shanzer; Z. I. Cabantchik *Anal. Biochem.* **1992**, *205*, 326-333.

11. Y.-H. Chan; Y. Jin; C. Wu; D. T. Chiu *Chem. Commun.* **2011**, *47*, 2820-2822.
12. J. P. Sumner; R. Kopelman *Analyst* **2005**, *130*, 528-533.
13. B. Wang; J. Hai; Z. Liu; Q. Wang; Z. Yang; S. Sun *Angew. Chem. Int. Ed.* **2010**, *49*, 4576-4579.
14. P. Suresh; I. A. Azath; K. Pitchumani *Sens. Actuators, B* **2010**, *146*, 273-277.
15. M.-C. Daniel; D. Astruc *Chem. Rev.* **2004**, *104*, 293-346.
16. N. L. Rosi; C. A. Mirkin *Chem. Rev.* **2005**, *105*, 1547-1562.
17. S.-P. Wu; Y.-P. Chen; Y.-M. Sung *Analyst* **2011**, *136*, 1887-1891.
18. R. Quinn; J. Mercer-Smith; J. N. Burstyn; J. S. Valentine *J. Am. Chem. Soc.* **1984**, *106*, 4136-4144.
19. P. O'Brien; D. A. Sweigart *Inorg. Chem.* **1985**, *24*, 1405-1409.
20. M. Y. M. Pau; M. I. Davis; A. M. Orville; J. D. Lipscomb; E. I. Solomon *J. Am. Chem. Soc.* **2007**, *129*, 1944-1958.
21. J. E. Bauman, Jr.; J. C. Wang *Inorg. Chem.* **1964**, *3*, 368-373.
22. W. Wu; J. Xie; D. Xie *Russ. J. Inorg. Chem.* **2010**, *55*, 384-389.
23. J. R. Wright; E. Frieden *Bioinorg. Chem.* **1975**, *4*, 163-175.
24. J. Wei; N. Teshima; S. Ohno; T. Sakai *Anal. Sci.* **2003**, *19*, 731-735.
25. A. Rigo; A. Corazza; M. L. di Paolo; M. Rossetto; R. Ugolini; M. Scarpa *J. Inorg. Biochem.* **2004**, *98*, 1495-1501.
26. C.-T. Kuo; Y.-M. Liu; S.-H. Wu; C.-H. Lin; C.-M. Lin; C.-h. Chen *Anal. Chem.* **2011**, *83*, 3765-3769.
27. J. M. Walshe *Am. J. Med.* **1956**, *4*, 487-495.
28. Y. Sugiura; H. Tanaka *Mol. Pharmacol.* **1972**, *8*, 249-255.
29. W. B. Herring; B. S. Leavell; L. M. Paixao; J. H. Yoe *Am. J. Clin. Nutr.* **1960**, *8*, 846-854.
30. A. A. Yunice, Serum Copper in Relation to Age. In *Ultratrace Metal Analysis in Biological Sciences and Environment*, Risby, T. H., Ed. American Chemical Society: Washington, DC, 1979; Vol. 172, p 240.
31. H. Vanhoe; C. Vandecasteele; J. Versieck; R. Dams *Anal. Chem.* **1989**, *61*, 1851-1857.
32. A. Bianconi *Appl. Surf. Sci.* **1980**, *6*, 392-418.
33. A. Bianconi; M. Dell'Aricecia; P. J. Durham; J. B. Pendry *Phys. Rev. B* **1982**, *26*, 6502-6508.
34. A. Gaur; B. D. Shrivastava; S. K. Joshi *J. Phys.: Conf. Ser.* **2009**, *190*, 012084.
35. Y. Nishida; K. Kino; S. Kida *J. Chem. Soc. Dalton Trans.* **1987**, 1157-1161.
36. C. Hu; B. C. Noll; C. E. Schulz; W. R. Scheidt *Inorg. Chem.* **2006**, *45*, 9721-9728.
37. S.-T. Wong; J.-F. Lee; S. Cheng; C.-Y. Mou *Appl. Catal. A* **2000**, *198*, 115-126.
38. F. Valach; M. Tokarčík; T. Maris; D. J. Watkin; C. K. Prout *J. Organomet. Chem.* **2001**, *622*, 166-171.
39. S. H. Laurie; E. S. Mohammed; D. M. Prime *Inorg. Chim. Acta* **1981**, *56*, 135-141.
40. F. Lambert; C. Policar; S. Durot; M. Cesario; L. Yuwei; H. Korri-Youssoufi; B. Keita; L. Nadjo *Inorg. Chem.* **2004**, *43*, 4178-4188.
41. F. Lambert; J.-P. Renault; C. Policar; I. Morgenstern-Badarau; M. Cesario *Chem. Commun.* **2000**, 35-36.
42. N. Matsumoto; Y. Mizuguchi; G. Mago; S. Eguchi; H. Miyasaka; T. Nakashima; J.-P. Tuchagues *Angew. Chem. Int. Ed. Engl.* **1997**, *36*, 1860-1862.

- 1
2
3
4
5
6
7
8
9
10
11
12
13
14
15
16
17
18
19
20
21
22
23
24
25
26
27
28
29
30
31
32
33
34
35
36
37
38
39
40
41
42
43
44
45
46
47
48
49
50
51
52
53
54
55
56
57
58
59
60
43. D. Zhao; J.-L. Shui; C. Chen; X. Chen; B. M. Reprogie; D. Wang; D.-J. Liu *Chem. Sci.* **2012**, *3*, 3200-3205.
44. R. Garrett; C. Grisham, *Biochemistry*. 5th; Mary Finch: Canada, 2012; p 41.
45. J. L. Wong; R. H. Sánchez; J. G. Logan; R. A. Zarkes; J. W. Ziller; A. F. Heyduk *Chem. Sci.* **2013**, *4*, 1906-1910.
46. S. G. Cohen *J. Am. Chem. Soc.* **1945**, *67*, 17-20.
47. P. Peng; G. Garnier *Langmuir* **2010**, *26*, 16949-16957.
48. L. G. Stadtherr; R. B. Martin *Inorg. Chem.* **1972**, *11*, 92-94.
49. T. Hirai; K. Fukushima; K. Kumamoto; H. Iwahashi *Biol. Trace Elem. Res.* **2005**, *108*, 77-85.
50. B. Alies; B. Badei; P. Faller; C. Hureau *Chem.–Eur. J.* **2012**, *18*, 1161-1167.
51. P. M. Henry *Inorg. Chem.* **1966**, *5*, 688.
52. G. F. Smith; W. H. McCurdy, Jr. *Anal. Chem.* **1952**, *24*, 371-373.
53. The selective reduction of Cu²⁺ by penicillamine can be manifested through the application of penicillamine as a copper chelator to treat the Wilson's disease^{27,28} induced by copper ions.
54. B. Huang; C. Chen *Free Radical Biol. Med* **2006**, *41*, 562-567.
55. L. M. Landino; M. T. Koumas; C. E. Mason; J. A. Alston *Biochem. Biophys. Res. Commun.* **2006**, *340*, 347-352.
56. G. Monteiro; B. B. Horta; D. C. Pimenta; O. Augusto; L. E. S. Netto *Proc. Natl. Acad. Sci. U.S.A.* **2007**, *104*, 4886-4891.
57. D. Giustarini; I. Dalle-Donne; R. Colombo; A. Milzani; R. Rossi *Nitric Oxide* **2008**, *19*, 252-258.